processes

MDPI

Article

Influence of Drilling Fluid Temperature, Density, and Salinity on Borehole Stability in Permafrost Strata

Yang Li [1,*], Jihui Shi [2], Qiang Cui [2] and Lifang Song [3]

[1] Sinopec Research Institute of Petroleum Engineering Co., Ltd., 197 Baisha Road, Changping District, Beijing 102200, China
[2] Sinopec Shanghai Offshore Oil & Gas Company, No. 1225, Shangcheng Road, Pudong New Area, Shanghai 200120, China
[3] School of Petroleum Engineering, China University of Petroleum (East China), No. 66, West Changjiang Road, Huangdao District, Qingdao 266580, China
* Correspondence: liyang_rock@163.com

Abstract: In the drilling process in permafrost strata, the mass and heat transfer effects may thaw the strata around the boreholes and decrease the content of pore ice, thus causing the mechanical properties of the strata to deteriorate greatly, thus influencing the stability of the borehole walls. In this work, a multiphysics coupling mathematical model was built for the stability of borehole walls in permafrost strata. Based on this model, the leading factors for the influences of the mass and heat transfer effects of drilling fluids on the stability of borehole walls were analyzed, and the influences of different drilling conditions on the stability of borehole walls were studied. The results demonstrate that the heat conduction of drilling fluids to the strata is the most important factor that influences the stability of borehole walls, and the diffusion of salt components affects the freezing temperature of pore water and the pore ice content in the frozen area. As the duration of the drilling increases, the collapsed zones of the borehole walls develop toward the radial and circumferential directions. Decreasing the temperature of the drilling fluids can improve the temperature distribution in the strata around the boreholes and is beneficial to reducing the degree of collapse. The increment in the concentration of salt components in the drilling fluids can decrease the overall temperature distribution in the strata, while the increase in the ionic concentration substantially decreases the pore ice content in permafrost and increases the borehole expansion rate. Enlarging the fluid column pressure of the drilling fluids does not intensify the mass and heat transfer effect of drilling fluids on the strata, while it greatly affects the stress distribution in the strata, shrinks the borehole collapse range, and improves the stability of the borehole walls.

Keywords: permafrost; stability of borehole wall; multiphysics coupling; mass and heat transfer

Academic Editor: Yidong Cai

Received: 13 December 2024
Revised: 7 January 2025
Accepted: 16 January 2025
Published: 21 January 2025

Citation: Li, Y.; Shi, J.; Cui, Q.; Song, L. Influence of Drilling Fluid Temperature, Density, and Salinity on Borehole Stability in Permafrost Strata. *Processes* **2025**, *13*, 297. https://doi.org/10.3390/pr13020297

1. Introduction

With the increasingly higher demand for fossil energy, the safe and efficient exploration and development technologies of unconventional oil and gas resources have become a focus in the current oil industry [1–3]. The exploration results of the United States Geological Survey in the circum-Arctic region reveal that abundant oil and gas resources are present in the permafrost in polar regions, which will become one of the supply sources of future oil and gas energy resources [4,5]. However, permafrost strata are characterized by low strength, undercompaction, and temperature sensitivity compared with conventional

strata [6,7]. Construction disturbance is very likely to cause the failure of the strata, with ensuing huge economic losses and engineering accidents. As reported by Vladimir, a series of problems, including the settlement of wellheads, the failure of borehole walls, and the slippage of production strings due to the thawing and collapse of soils around boreholes, occurred during drilling and development in the Zapolyarnoye gas field [8,9]. Therefore, studying the possible geomechanical problems during construction in permafrost strata is the basic precondition and technical support for guaranteeing successful oil and gas development in polar regions.

When drilling boreholes in permafrost strata, the mass and heat transfer effects between the drilling fluids and strata will cause the thawing and chemical decomposition of the pore ice around the boreholes, change the mechanical properties and stress distribution of the strata, and lead to the failure of borehole walls [10]. Because drilling technologies in permafrost strata are still under exploration, researchers have mainly conducted relevant studies on the mechanical evolution characteristics of the strata around boreholes and the influences of the heat transfer effect of fluids on strata in the drilling process. For example, Perkins (1974) proposed that the secondary freezing of strata increases the strata pressure and damages casing pipes by analyzing the distribution characteristics of the stress around the boreholes in permafrost after freezing and thawing cycles in the drilling process [11]. Wang (2015) used fast Lagrangian analysis of continua (FLAC) to analyze the influencing factors of the minimum wellbore pressure in the drilling process in permafrost strata. The regression analysis of the results indicates that the minimum wellbore pressure is a function of the pore pressure, cohesion, internal friction angle, temperature difference, heat transfer time, and wellbore radius [12]. By establishing the coupling model of heat transfer for wellbores and strata, Wang (2017) analyzed the influences of the heat transfer effect of drilling fluids on the temperature field in strata. Changes in the heat transfer performance of permafrost and the phase-change latent heat of pore ice were reported to decrease the heat transfer efficiency in permafrost [13]. According to the temperature distribution characteristics in permafrost during drilling, Kutasov (2017) proposed a temperature logging method for determining the secondary freezing time after the thawing of strata around boreholes [14]. Li (2019) analyzed the influences of the temperature of drilling fluids on the plastic yield zone around the boreholes in the drilling process in permafrost strata. In this way, the phase change in the pore ice in permafrost was reported to seriously alter the mechanical properties of the permafrost, which caused the permafrost to have a lower elastic modulus and a lower strength, rendering a larger area of the strata into the plastic yield zone [15]. By analyzing the heat transfer properties and the distribution characteristics of the phase change interface in permafrost strata, Eppelbaum (2019) proposed a method for calculating the evolution of the thawing range of permafrost in the following two operation modes: drilling and well shutdown [16]. Li (2020) analyzed the borehole evolution under the conditions of different immersion times in drilling fluids and the temperatures of the drilling fluids. Li (2020) also stated that plastic deformation in the strata around the boreholes accumulates constantly with a prolonged drilling duration. When the strata temperature is high, high-temperature drilling fluids are suggested to accelerate the drilling; if the strata temperature is low, low-temperature drilling fluids should be used to maintain the stability of the boreholes [10].

The above studies have analyzed the engineering problems encountered in drilling operations in permafrost strata, mainly from the perspectives of mechanics and heat transfer theory. These studies ignore the influences of an important factor, that is, the mass transfer effect of drilling fluids on the strata. While drilling boreholes in permafrost strata, many ionic salts are generally added to the drilling fluids to avoid the freezing of the fluids in the low-temperature environments [17,18]. The heat and salt components in

the drilling fluids transfer to the strata through conduction, diffusion, and convection, thus changing the distributions of the temperature field, pore pressure field, chemical field, and stress field in the strata. The stability of borehole walls is the result of the joint action of multiple factors [19,20]. Existing research shows that, when the mass transfer effect of the drilling fluids affects the physical properties of the strata, ignoring this factor may cause the evaluation results of the stability of the borehole walls to deviate substantially from reality, as exemplified by the hydration of shale [21,22] and the decomposition of hydrate layers [23–25]. Therefore, the mechanical responses of borehole walls in permafrost are a result of the joint action of the mass and heat transfer of the drilling fluids. According to the mass and heat transfer characteristics of drilling fluids to the strata during drilling, a thermohydrosolid–chemical multiphysics coupling mathematical model that meets the drilling conditions in permafrost strata was built. In addition, a mechanical model of permafrost at different temperatures was established by performing low-temperature triaxial mechanical tests. On this basis, the leading factors for the influences of the mass and heat transfer effects of drilling fluids during drilling in permafrost strata on the stability of borehole walls were analyzed. Moreover, the mechanical mechanisms underlying the influences of different drilling durations, as well as the different temperatures, salinities, and densities of drilling fluids on the stability of borehole walls, were studied.

2. Mathematical Model

2.1. Governing Equations for Mass and Heat Transfer in Permafrost Strata

The analysis of the influences of the mass and heat transfer effects of drilling fluids on the stability of borehole walls in permafrost strata involves the seepage mechanics, heat transfer theory, dilute material transfer, and solid mechanics of the permafrost strata. Therefore, the basic governing equations and parametric equations needed in the calculation are established in this section, and COMSOL Multiphysics 6.1 (COMSOL Inc., Stockholm, Sweden) is used for the modeling and analysis.

2.1.1. Governing Equation for Seepage in Permafrost Strata

According to the law of the conservation of mass, the flow of unfrozen water in permafrost follows the conservation equation of mass, as displayed in Equation (1):

$$\nabla \cdot (\rho_w v) + \frac{\partial(\rho_w \phi_e)}{\partial t} = -\phi_0 \rho_i \frac{\partial S_i}{\partial t} \tag{1}$$

where ρ_w, v, ϕ_e, t, ρ_i, and S_i represent the fluid density (kg/m^3), seepage velocity of the fluids (m/s), effective porosity of the soils, time (s), density of the pore ice (kg/m^3), and volume saturation of the pore ice, respectively. The equation means that the mass change in the unfrozen pore water in an enclosed surface area of microunits is equal to the sum of the mass difference in the inflow and outflow within the same interval, and the mass of the pore ice that is thawed to pore water; ϕ_0 denotes the initial porosity of the strata.

The motion equation of the unfrozen pore water follows Darcy's law of seepage, as shown in Equation (2):

$$v_w = -\frac{k}{\mu} \nabla(p) \tag{2}$$

where k, μ, p, and v_w represent the permeability of soils (mD), fluid viscosity ($mPa \cdot s$), pore pressure (MPa), and seepage velocity of fluids (m/s), respectively.

The elastic porous medium state equation is shown in Equation (3), as follows:

$$\phi_e = S_w \phi_0 + C_f (p - p_0) \tag{3}$$

where S_w, C_f, and p_0 indicate the volume saturation of unfrozen pore water, compressibility of soils (MPa^{-1}), and initial pore pressure (MPa), respectively.

For unfrozen pore water, its state equation can be expressed as Equation (4) according to the Maclaurin expansion, as follows:

$$\rho_w = \rho_{w0}[1 + C_1(p - p_0)] \tag{4}$$

where ρ_{w0} denotes the fluid density (kg/m^3) under pressure p_0 and C_1 represents the compressibility of fluids (MPa^{-1}).

By substituting Equations (2)–(4) into Equation (1) and ignoring the higher-order term, the following results shown in Equation (5) can be obtained:

$$(1 - \frac{\rho_i}{\rho_{w0}} + C_1 p)\frac{\partial S_w}{\partial t} + (C_1 S_w + \frac{C_f}{\phi_0})\frac{\partial p}{\partial t} = \frac{k}{\phi_0 \mu}\nabla(p) \tag{5}$$

When the permafrost is completely thawed ($S_w = 1$), Equation (5) degenerates into Equation (6), as follows:

$$(\phi_0 C_1 + C_f)\frac{\partial p}{\partial t} = \frac{k}{\mu}\nabla(p) \tag{6}$$

This equation is the same as the differential equation used for unsteady seepage flows of single-phase microcompressible fluids in conventional elastic porous media.

If the compressibility of rocks and fluids is not considered ($C_1 = C_f = 0$), Equation (5) degenerates into Equation (7), as follows:

$$(1 - \frac{\rho_i}{\rho_{w0}})\frac{\partial S_w}{\partial t} = \frac{k}{\phi_0 \mu}\nabla(p) \tag{7}$$

This equation is the same as the differential equation of seepage in permafrost strata proposed by Harlan (1973) [26].

2.1.2. Heat Transfer Equations of Permafrost Strata

Heat transfer in permafrost strata abides by the law of the conservation of energy. That is, the sum of heat produced by heat conduction and convection in an enclosed surface area of microunits is equal to the sum of the heat difference in the inflow and outflow within the same interval, and the phase-change latent heat absorbed during the thawing of pore ice into pore water, where

$$c_f \rho_f \frac{\partial T}{\partial t} + \rho_w c_w \nabla \cdot (v_w T) = \nabla(\lambda_f \nabla T) + \phi_0 L \rho_i \frac{\partial S_i}{\partial t} \tag{8}$$

c_f and c_w refer to the heat conduction coefficients of permafrost and water, respectively ($J/(kg \cdot {}^\circ C)$); ρ indicates the density of the permafrost (kg/m^3); λ_f denotes the heat conduction coefficient of the permafrost ($W/(m \cdot {}^\circ C)$); L represents the latent heat of the ice–water phase change (J/kg).

2.1.3. Transfer Equation of Dilute Materials

If there are ionic additives in the drilling fluids, the ions diffuse to the strata due to the seepage of the drilling fluids and the action of the potential difference in the concentration. The governing equation can be expressed as Equation (9) [27], as follows:

$$\frac{\partial J_k}{\partial t} + \nabla \cdot (-D_k \nabla J_k) + v_w \nabla J_k = 0 \tag{9}$$

where J_k denotes the ionic concentration (mol/L) and D_k represents the ionic diffusion coefficient (m^2/s).

2.1.4. Equation in Solid Mechanics

When considering the action of pore pressure on the deformation field of strata, the stress–strain equilibrium equation of the microunits of strata can be expressed as Equation (10) according to the principle of effective stress [28], as follows:

$$\sigma_{ij} + f_i - (\alpha \delta_{ij} p)_{,i} = 0 \tag{10}$$

where f_i, σ_{ij}, and α represent the load component of the body force, stress component of microunits of the strata, and the effective stress factor, respectively; δ_{ij} denotes the Kronecker symbol, and $\delta_{ij} = [1 \quad 1 \quad 1 \quad 0 \quad 0 \quad 0]^T$.

The geometric equation for permafrost strata is shown as Equation (11), as follows:

$$\varepsilon_{ij} = \frac{1}{2}(u_{i,j} + u_{j,i}) \tag{11}$$

where ε_{ij} and $u_{j,i}$ represent the strain component and displacement component, respectively.

When the elastic–plastic model is used to characterize the stress–strain characteristics of soils, the elastic–plastic constitutive equation can be expressed as Equation (12), as follows:

$$\{d\sigma\} = [D_{ep}]\{d\varepsilon\} \tag{12}$$

where $d\sigma$ and $d\varepsilon$ denote the stress increment and strain increment, respectively, and D_{ep} represents the elastic–plastic matrix of permafrost, which is determined by the plastic matrix and elastic matrix, $[D_{ep}] = [D_e] - [D_p]$.

The pore pressure of the strata can be calculated using Equation (13), as follows:

$$p = \rho_w g h \tag{13}$$

where g denotes the gravitational acceleration (m/s^2) and h represents the depth of the strata (m).

The overburden pressure of the strata can be calculated using Equation (14), as follows:

$$\sigma_v = \rho_f g h \tag{14}$$

Because the strata are buried shallowly, the tectonic stress is low, and the maximum and minimum horizontal geostresses can be separately calculated using Equations (15) and (16), as follows:

$$\sigma_h = \frac{\mu}{1-\mu}\sigma_v \tag{15}$$

$$\sigma_H = l\sigma_h \tag{16}$$

where σ_v denotes the overburden pressure (MPa); σ_h and σ_H represent the minimum and maximum horizontal geostresses (MPa), respectively; μ indicates Poisson's ratio; l represents the coefficient of the horizontal geostress ratio, which is valued as 1.1.

2.2. Equations for the Physical Parameters of Permafrost Strata

2.2.1. Seepage and Heat Transfer Equations

When the ambient temperature is below the freezing temperature of pore water, some of the pore water is frozen to pore ice and, therefore, becomes immobile, thus reducing the permeability of the soils. Therefore, the permeability of the permafrost is related to the content of unfrozen water and can be expressed as Equation (17) [29], as follows:

$$k = k_i / I \tag{17}$$

where k_i represents the permeability of soils that do not contain pore ice (mD) and I denotes the resistance coefficient of ice ($I = 10^{10^{\theta_i}}$).

The saturation of unfrozen water in soils is related to the ambient temperature and the salt concentration, and the saturation of unfrozen water in soils can be calculated using Equation (18) [30], as follows:

$$S_w = \left(\frac{T_0 - T_{f0} + K_{fC}\sum_k J_k}{T_0 - T}\right)^b \tag{18}$$

where T_0 denotes the freezing temperature of pure water and is valued as 0 °C; T_{f0} represents the freezing temperature of pore water in soils (°C), and is related to the ionic concentration and $T_{f0} = -0.0462 - 3.7308 J_k$ for the NaCl solution; K_{fC} indicates the reduction coefficient of the freezing temperature expressed by the molar concentration, and is 1.85 $°C/(mol \cdot L^{-1})$; J_k represents the molar concentration of the kth ion (mol/L); b is an experimental parameter that is related to the ionic concentration, and is $b = -1.5445 J_k^2 + 1.9197 J_k + 0.6412$ for the NaCl solution.

According to the volume saturation of pore water, the calculation equation for the saturation of pore ice is shown as Equation (19), as follows:

$$S_i = 1 - S_w \tag{19}$$

2.2.2. Physical Parameters of Heat Transfer

As the temperature changes, the content of unfrozen pore water in soils also varies, thus changing the heat conductivity and the specific heat capacity of the soils. Therefore, the heat conductivity of permafrost at a certain temperature is expressed as Equation (20) [10], as follows:

$$\lambda_f = \lambda_w^{\phi_0 S_w} \lambda_i^{\phi_0 S_i} \lambda_s^{1-\phi_0} \tag{20}$$

where λ_w, λ_i, and λ_s represent the heat conduction coefficients of water, ice, and the soil skeleton, respectively.

The specific heat capacity of permafrost can be represented as Equation (21), as follows:

$$c_f = \frac{\phi_0(S_w \rho_w c_w + S_i \rho_i c_i) + (1 - \phi_0)\rho_s c_s}{\phi_0(S_w \rho_w + S_i \rho_i) + (1 - \phi_0)\rho_s} \tag{21}$$

where c_w, c_i, and c_s denote the specific heat capacities of water, ice, and the soil skeleton, respectively.

2.3. Mechanical Parameters

The mechanical properties and strength criteria of the permafrost strata under different drilling conditions are the preconditions for judging the mechanical stability of the borehole walls. Natural permafrost in Mohe city, Heilongjiang Province, China, was reproduced in the laboratory by simulating the underground environment, and a low-temperature triaxial mechanical test was conducted. The stress–strain characteristics of the permafrost were described using the ideal elastic–plastic constitutive model and the Mohr–Coulomb plasticity criterion. The test devices and test results are shown in Figure 1. The test results reveal that the initial elastic modulus of the permafrost samples gradually increases as the temperature declines. The Poisson's ratio of the permafrost samples fluctuates irregularly between 0.32 and 0.38. At the same temperature, the strength of the permafrost samples gradually increases as the confining pressure rises; under the same confining

pressure, the strength of the permafrost samples grows substantially with the decrease in the temperature, so that the cohesion and internal friction angle gradually increase with the decreasing temperature of the samples. Therefore, the elastic modulus, yield strength, and internal friction angle of permafrost samples can be calculated using Equations (22)~(24), and the Poisson's ratio is 0.35, as follows:

$$E = E_0 + f_1(T) = E_0 + a_1 T + a_2 T^2 \tag{22}$$

$$c = c_0 + f_2(T) = c_0 + a_3 T + a_4 T^2 \tag{23}$$

$$\varphi = \varphi_0 + f_3(T) = \varphi_0 + a_5 T + a_6 T^2 \tag{24}$$

where c, φ, and E, respectively, represent the cohesion (MPa), internal friction angle (°), and elastic modulus (MPa) of the permafrost; c_0, φ_0, and E_0 separately denote the cohesion (MPa), internal friction angle (°), and elastic modulus (MPa) of the thawed soils; a_1, a_2, a_3, a_4, a_5, and a_6 are the fitting parameters in the test; f is a function pertaining to the temperature.

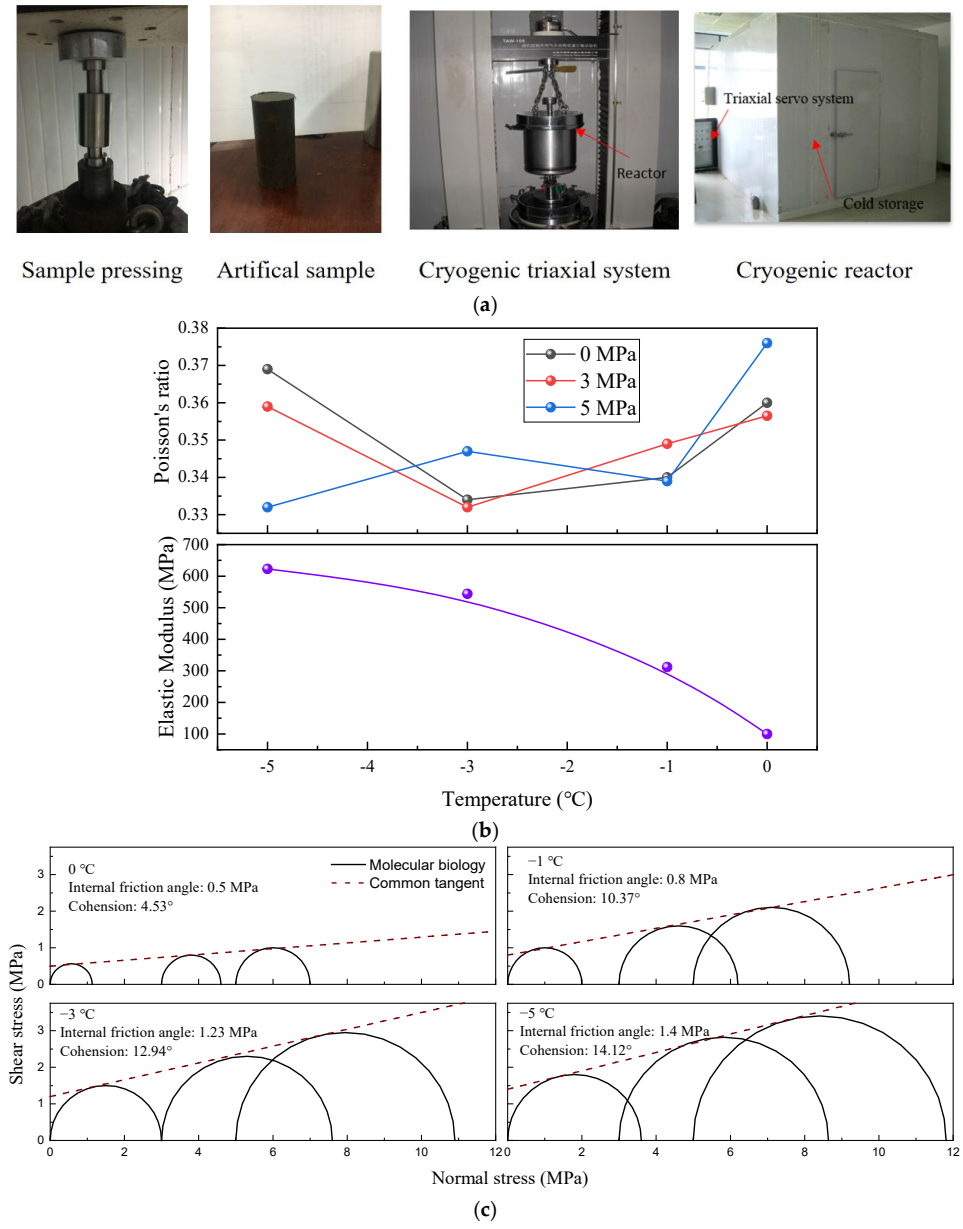

Figure 1. The low-temperature triaxial mechanical test and test results. (**a**) The test devices. (**b**) The test results of the elastic parameters. (**c**) The test results of the yield strength.

Based on the correlation between the saturation of unfrozen water in the permafrost and the ambient temperature under conditions without ionic salts, the relationships of the cohesion, internal friction angle, and elastic modulus with the saturation of unfrozen water can be further obtained, as shown in the following Equations (25)~(27):

$$E = E_0 + f_3(T_0 - \frac{T_0 - T_{f0}}{S_w^{\frac{1}{b}}}) \tag{25}$$

$$c = c_0 + f_1(T_0 - \frac{T_0 - T_{f0}}{S_w^{\frac{1}{b}}}) \tag{26}$$

$$\varphi = \varphi_0 + f_2(T_0 - \frac{T_0 - T_{f0}}{S_w^{\frac{1}{b}}}) \tag{27}$$

3. Verification and Establishment of Models

3.1. Model Verification

To ensure the accuracy of the established models, the established models are verified in this section, which can be divided into two parts. The first part is to verify the thermohydrosolid coupling model in the injection process of low-temperature fluids, and the second part is to validate the freezing model of permafrost considering the phase-change process.

3.1.1. Verification of the Thermohydrosolid Coupling Model in the Drilling Process

The model to be verified has a borehole with a radius of 0.1 m in an infinite stratum with an initial temperature of 200 °C. Fluids of 80 °C were injected through the borehole to analyze the evolution of the strata temperature, pore pressure, and stress in the process. The numerical calculation results are compared with the analytical solution to verify the accuracy of the thermohydrosolid coupling model. The numerical model and boundary conditions are shown in Figure 2a. The specific parameters needed for the calculation refer to previous research (Ghassemi 2004). Figure 2b compares the calculation results of the analytical solution and the numerical model. Their error can be seen to be less than 1%, so the established model can be used to characterize the mass and heat transfer effects between the drilling fluids and strata and the mechanical stability in the drilling process [31].

3.1.2. Verification of the Freezing Model of Permafrost

The validation model is a soil sample with a height and diameter both of 100 mm. The initial temperature is 1.5 °C, and constant-temperature boundary conditions of −1.6 and 1.5 °C are separately applied on the upper and lower surfaces to analyze the temperature evolution of the soil sample in the freezing process of the lower surface. The geometric model and boundary conditions of the numerical model are displayed in Figure 3a. The calculation parameters of the validation model are set by referring to previous research (Li et al., 2018). Figure 3b,c illustrate the calculation results of the permafrost temperature field using the model. By comparing the experimental results obtained by Li, the maximum error between the calculation results and the experimental results can be seen to be found at measurement point P1 after drilling for 13 h. The two have an error of 0.39 °C, which is 12.58% of the whole temperature range. Considering the error during the experimental measurement, the established mathematical model is deemed accurate and can be used to calculate the evolution of the permafrost temperature field in the phase-change process [32].

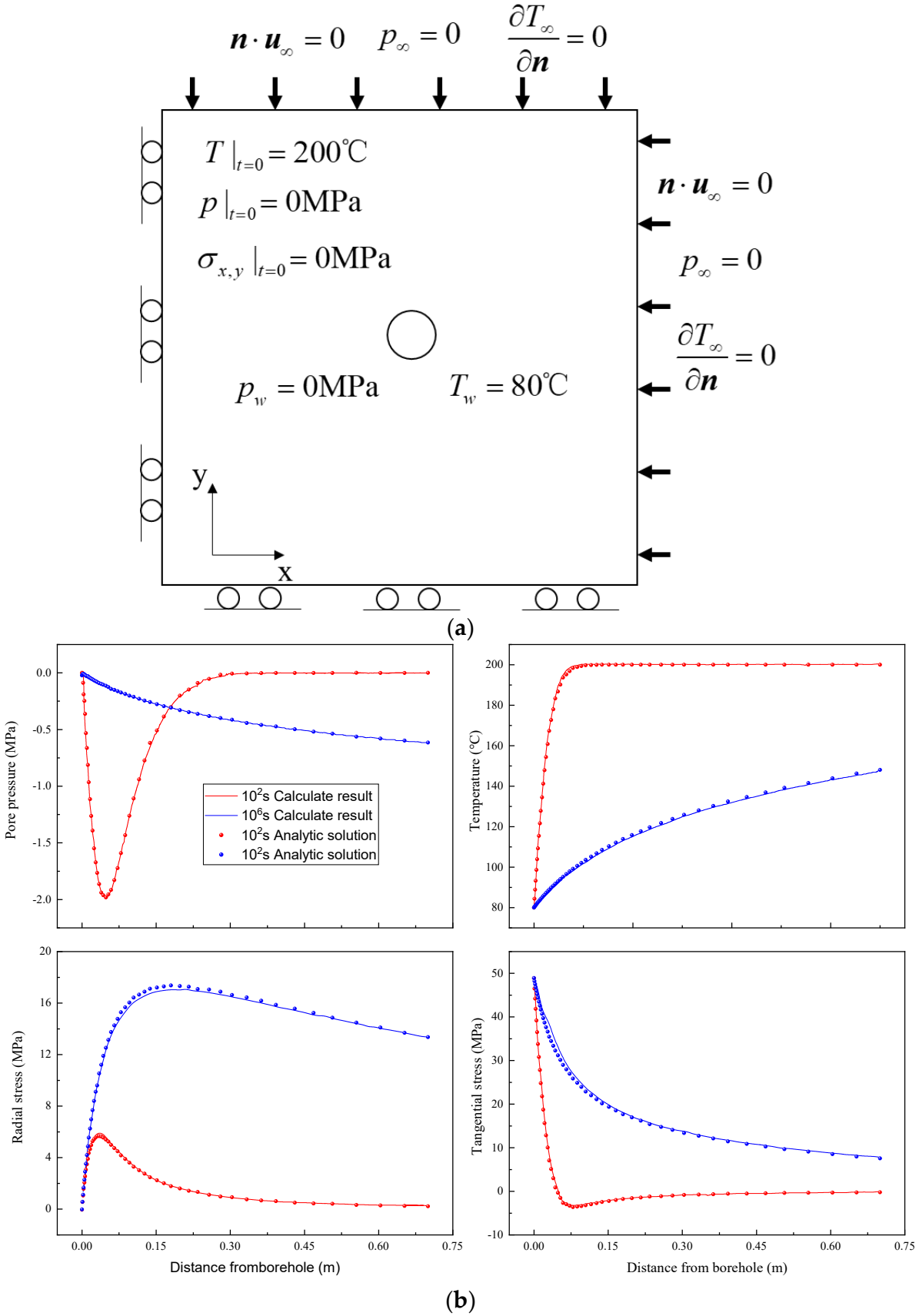

Figure 2. The thermohydrosolid coupling model and result analysis. (**a**) The thermohydrosolid coupling model in the injection process of low-temperature fluids. (**b**) Comparison of the calculation results of the analytical solution and numerical model.

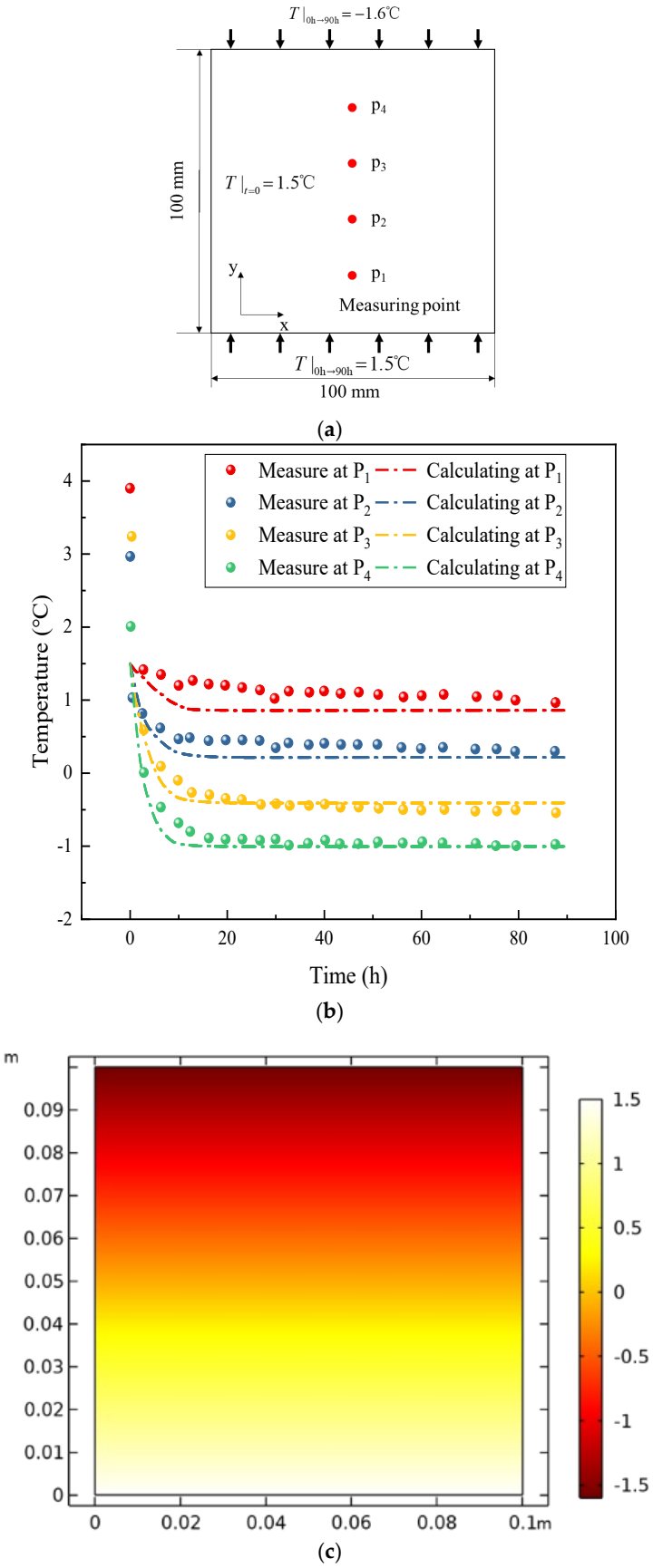

Figure 3. Verification of the permafrost temperature field model. (**a**) The geometric model and boundary conditions. (**b**) Comparison between the experimental results and calculation results at the measurement points. (**c**) Temperature distribution after 90 h.

3.2. Numerical Model for Stability of Borehole Walls in Permafrost Strata

According to the drilling conditions in permafrost strata, the analysis model for the stability of borehole walls in permafrost strata can be built, as shown in Figure 4. The geometric model is composed of a round outer boundary with a diameter of 20 m and a borehole with a diameter of 1.32 m. On the outer boundary, the boundary conditions of the displacement constraint, pore pressure equal to the strata pressure, and outflow ions and temperature are applied. On the inner boundary, the load equal to the fluid column pressure of the drilling fluids and the pore pressure are applied as the boundary conditions. In addition, the temperature boundary conditions equal to the temperature of the drilling fluids, and the concentration boundary conditions identical to the concentration of the salt components in the drilling fluids are also applied. Moreover, the initial temperature field, the initial pressure field of the strata, the initial concentration field (0 mol/L) of the salt components, and the initial stress field are applied to the whole model as well. The calculation parameters of the model are listed in Table 1.

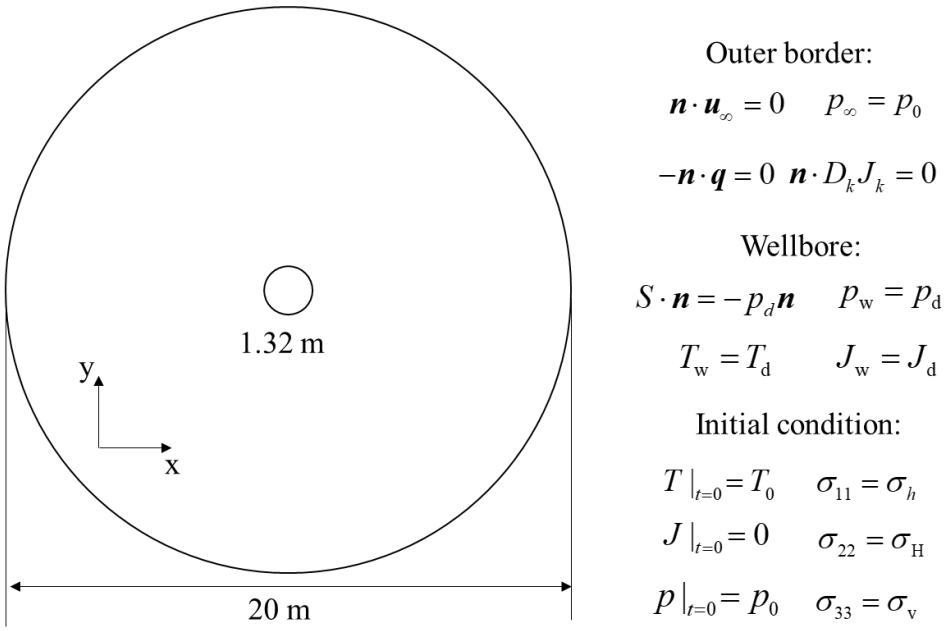

Figure 4. Geometric model for the stability of the borehole walls in the permafrost strata and its boundary conditions.

Table 1. Numerical calculation parameters [10].

Parameter	Value	Unit	Parameter	Value	Unit
Heat conductivity of water	0.55	$W{\cdot}m^{-1}{\cdot}K^{-1}$	Internal friction angle of thawed soils	5.1786	°
Heat conductivity of ice	2.22	$W{\cdot}m^{-1}{\cdot}K^{-1}$	Parameter a_1	−22.813	
Heat conductivity of soils	1.383	$W{\cdot}m^{-1}{\cdot}K^{-1}$	Parameter a_2	−216.96	
Specific heat capacity of water	4200	$J{\cdot}kg^{-1}{\cdot}K^{-1}$	Parameter a_3	−0.0274	
Specific heat capacity of ice	1930	$J{\cdot}kg^{-1}{\cdot}K^{-1}$	Parameter a_4	−0.3158	
Specific heat capacity of soils	982	$J{\cdot}kg^{-1}{\cdot}K^{-1}$	Parameter a_5	−0.5589	
Water density	1000	kg/m^3	Parameter a_6	−4.534	
Ice density	920	kg/m^3	Depth of strata	500	m
Soil density	2650	kg/m^3	Initial strata temperature	−5	°C
Phase-change latent heat of water	334	kJ/kg	Initial strata pressure	4.9	MPa
Initial permeability of soils	1×10^{-8}	m^2	Overburden pressure	9.80	MP
Initial porosity of soils	0.37		Maximum horizontal geostress	7.11	MPa
Compressibility of water	4.9×10^{-4}	MPa^{-1}	Minimum horizontal geostress	5.80	MPa
Compressibility of ice	4.5×10^{-4}	MPa^{-1}	Initial ionic concentration	0	mol/L
Compressibility of soils	1.5×10^{-4}	MPa^{-1}	Density of drilling fluids	1.03	kg/m^3
Elastic modulus of thawed soils	106.21	MPa	Temperature of drilling fluids	10	°C
Cohesion of thawed soils	0.504	MPa	Ionic concentration of drilling fluids	0.5	mol/L

4. Influences of the Mass and Heat Transfer Effects of Drilling Fluids on the Stability of Borehole Walls

To analyze the influences of the mass transfer effect on the stability of the borehole walls in the drilling process in permafrost strata, three models were established at the same time for comparison. Model 1 considers the influences of the heat conduction, diffusion of the salt components, and convective term; Model 2 considers the influences of the heat conduction and diffusion of the salt components; Model 3 considers only the effect of heat conduction, and the temperature of the high-temperature drilling fluids is 10 °C.

Figure 5 shows the distributions of the strata temperature around the boreholes, the ice saturation, the pore pressure, and the concentration of salt components after drilling for 10 h, calculated using the three models. As shown, when only the heat conduction is considered, the temperature propagates the fastest, and declines from the borehole walls to the strata far from the borehole. If the mass transfer effect of the salt components in the strata is also considered (Model 1 and Model 2), the temperature propagation in the strata near the boreholes lags behind, and the temperature first decreases and then increases. The lowest temperature is found in the strata 0.51 m from the borehole walls, at −6.2 °C, which is lower than the initial strata temperature. However, the pore ice content in the strata around the boreholes is lower than the pore ice content in the strata around the boreholes in Model 1, as shown in Figure 5b, because, when considering the transfer of salt components from the boreholes to the strata, the concentration changes in the ionic salts in the pores causes the chemical decomposition of some of the pore ice at low temperatures, which absorbs heat, as displayed in Figure 5c. After 10 h, the salt components in the drilling fluids have affected the strata 0.75 m around the boreholes, so that the strata temperature within 1.2 m from the borehole is influenced by the mass transfer effect of the salt components.

At the same time, the calculation results of the distributions of the strata temperature, pore ice, and salt concentration when considering, or not considering, the convective term (Model 1 and Model 2) differ slightly, because the transfer of heat and dilute materials via convection relies on the flow of fluids in the strata. Although a certain amount of unfrozen water is present in the permafrost, and the pore ice content near the boreholes decreases due to the influences of the drilling fluids, the permeability and porosity in the strata far from the boreholes still remain extremely low (Figure 6a,b). Therefore, the fluids in the strata flow at an extremely low rate. Figure 6b illustrates the distribution of the pore pressure in the strata, from which it can be seen that the differential pressure that drives the migration of fluids occurs mainly in the zone of extremely low permeability. Therefore, the heat transfer of the drilling fluids to the permafrost strata is dominated by heat conduction, and the transfer of salt components is dominated by molecular diffusion, while convection hardly plays any role. As shown in Figure 7, the boundary heat flux of heat conduction at the borehole walls is in the order of magnitude of 10^3 W/m, which is far higher than the boundary heat flux of heat conduction at the borehole walls produced by heat convection. In addition, the diffusion flux in the transfer of dilute materials is also far higher than the convection flux.

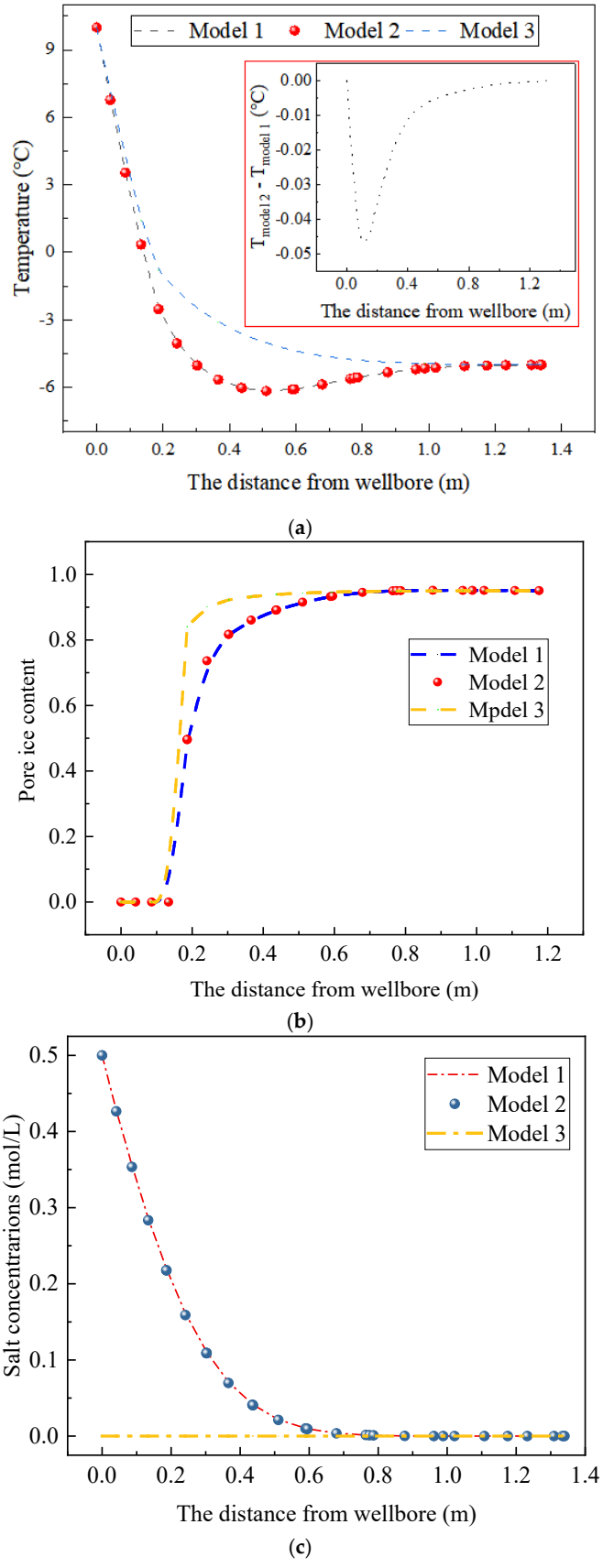

Figure 5. The distributions of the strata temperature, ice saturation, and salt concentration around the boreholes after drilling for 10 h obtained by the three models. (**a**) Distribution of the strata temperature around the boreholes. (**b**) Distribution of the pore ice content in the strata around the boreholes. (**c**) Distribution of the salt concentrations around the boreholes.

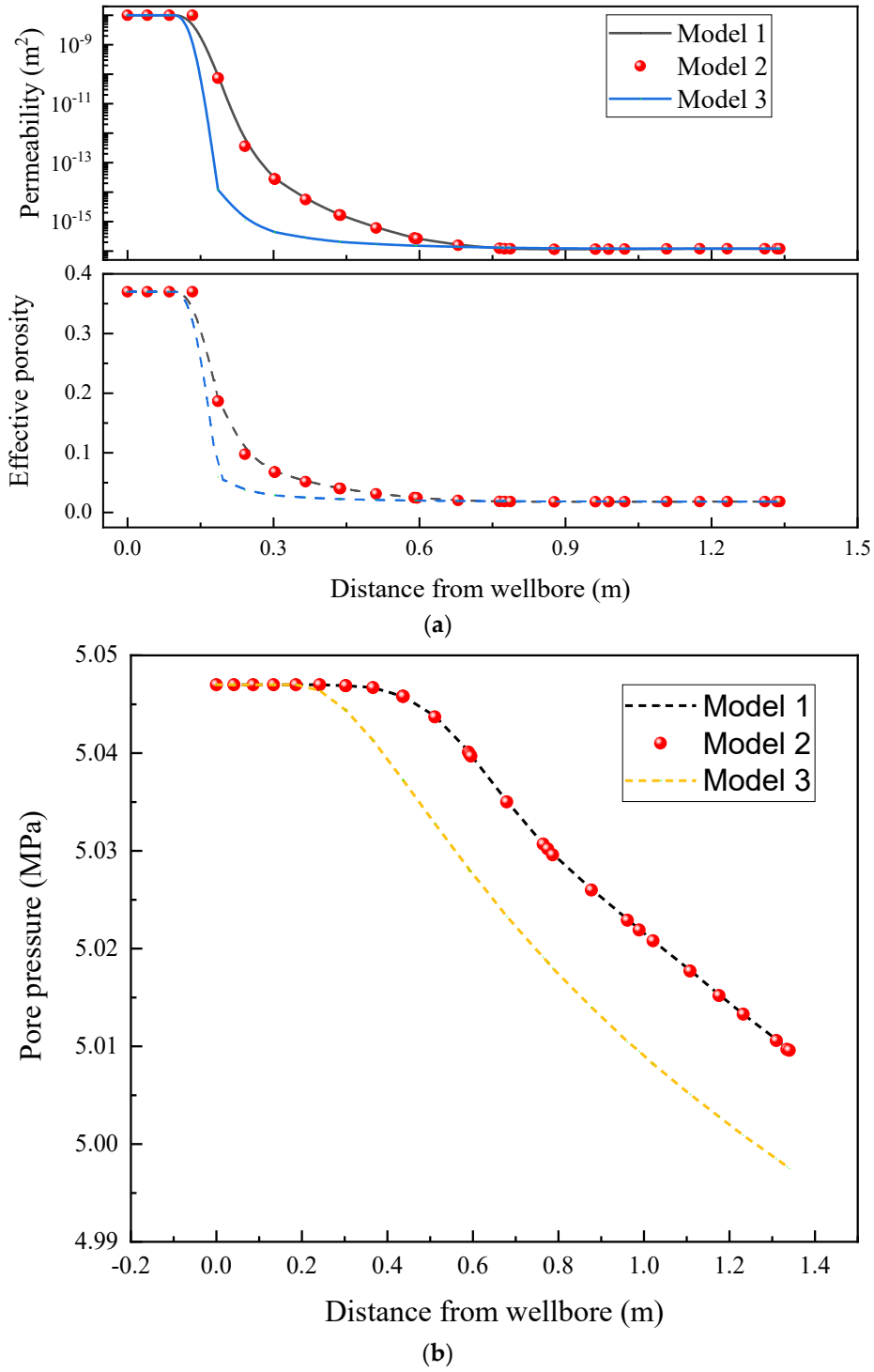

Figure 6. Distribution curves of the seepage parameters of the strata when drilling with high-temperature drilling fluids. (**a**) Distribution of the physical parameters of the strata. (**b**) Distribution of the pore pressure of the strata.

Figure 8 shows the cloud pictures for the distributions of the mechanical parameters of the strata after drilling the borehole for 10 h obtained by the three models (for the sake of clear observation, the strata near the boreholes are amplified). The mass and heat transfer effects of the drilling fluids greatly weaken the elastic modulus and cohesion of the strata near the boreholes, thus causing the plastic yield and collapse of the strata around the boreholes. If only the heat conduction effect of the drilling fluids is considered, the calculated weakened zone of the strata is obviously smaller than the calculated weakened

zone of the strata obtained in Model 1 and Model 2, as shown in Figure 9. When taking a plastic strain of 0.03 as the critical collapse strain, the prediction result of Model 3 for the collapsed zone is smaller. For example, Model 1 and Model 2 predict that the borehole expands by 24.2% in the direction of the minimum horizontal geostress, while the borehole expands by 16.7% when using Model 3 for the prediction.

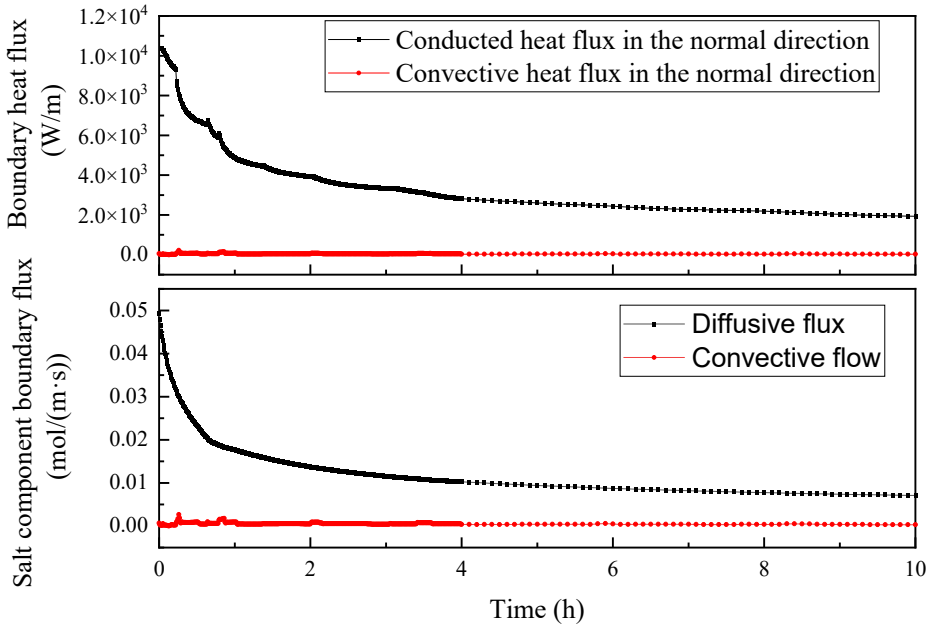

Figure 7. Change curves of the boundary flux in Model 1.

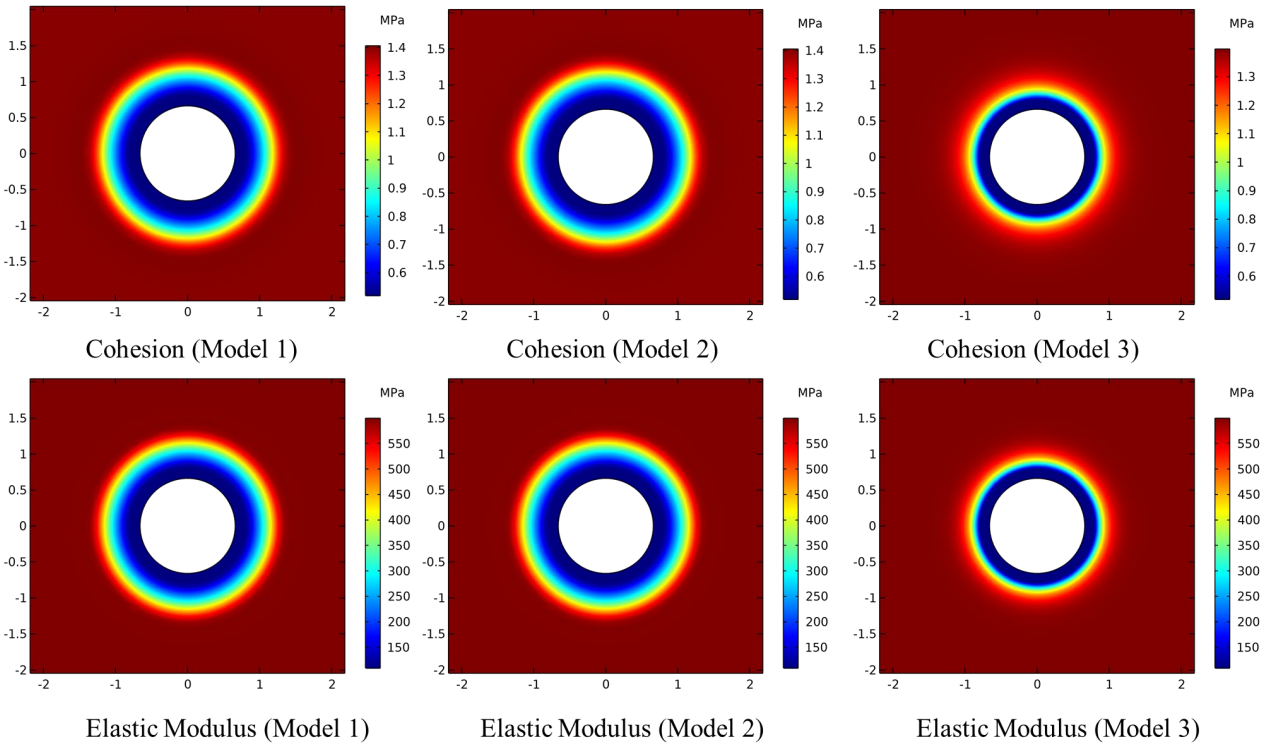

Figure 8. Cloud pictures for the distribution of the mechanical properties of the strata drilled with high-temperature drilling fluids.

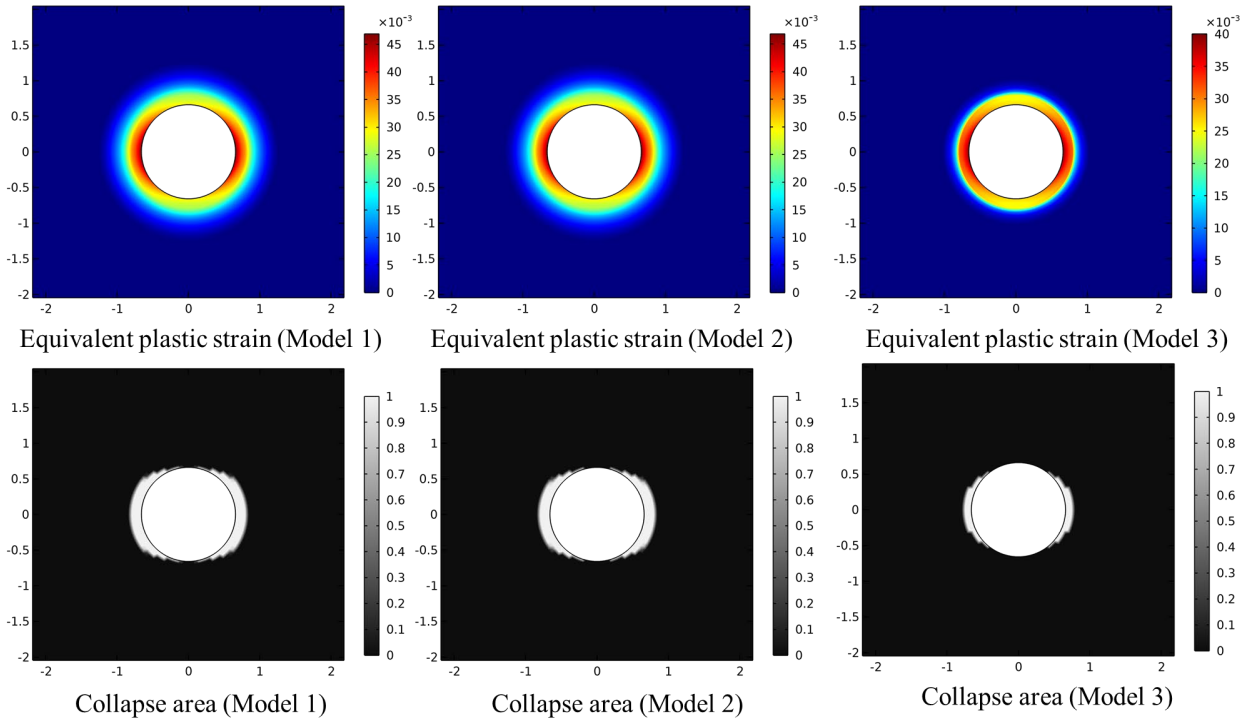

Figure 9. Cloud pictures for the distributions of the equivalent plastic strain and collapse range in the strata drilled with high-temperature drilling fluids.

Therefore, when analyzing the influencing factors of high-temperature drilling fluids on the stability of borehole walls in permafrost strata, the most important factor is the heat conduction of the drilling fluids with the strata, which directly determines the thawing range of the permafrost. This factor is followed by the mass transfer effect of the salt components in the drilling fluids on the strata. The diffusion of the salt components affects the freezing temperature of the pore water and the pore ice content in the frozen area, thus changing the mechanical properties of the frozen strata. If this factor is ignored, the collapse range of the boreholes will be seriously underestimated. Limited by the seepage performance of frozen strata, the convective term has only an extremely small influence on the mass transfer, heat transfer, and stability of the borehole walls (which is completely different from the hydrate strata and other temperature-sensitive strata) [27]. Therefore, the convective term can be ignored in practical modeling.

5. Influences of Different Factors on the Stability of Borehole Walls in Permafrost Strata

In the practical drilling process, reasonable drilling schemes should be designed according to different geological characteristics to reduce the failure risk of borehole walls as much as possible. Therefore, exploring the influences of different factors on the stability of borehole walls is the precondition and basis. Thus, this section carries out a sensitivity analysis on the influences of different drilling durations as well as different temperatures, densities, and salinities of drilling fluids on the stability of borehole walls.

5.1. Influences of Drilling Durations

Figure 10 shows the distributions of the temperature field, chemical field, and mechanical properties of the strata around the boreholes after different drilling durations. With the increase in the drilling duration, the zone affected by the mass and heat transfer effects of the drilling fluids can be seen to enlarge in the strata. For example, the strata 0.06 m from the borehole walls are thawed, the temperature field within 0.36 m from the borehole walls

is affected by the heat transfer of the drilling fluids, and the affected range of the chemical field is 0.27 m from the borehole walls after drilling for 1 h. After drilling the borehole for 10 h, the thawing range of the strata enlarges to 0.15 m, and the affected range of the chemical field also increases to 0.8 m from the borehole walls. The increase in the affected range of the temperature field and the chemical field in the strata enlarges the area of the strata with reduced mechanical properties around the boreholes, thus leading to a greater failure risk in the borehole walls.

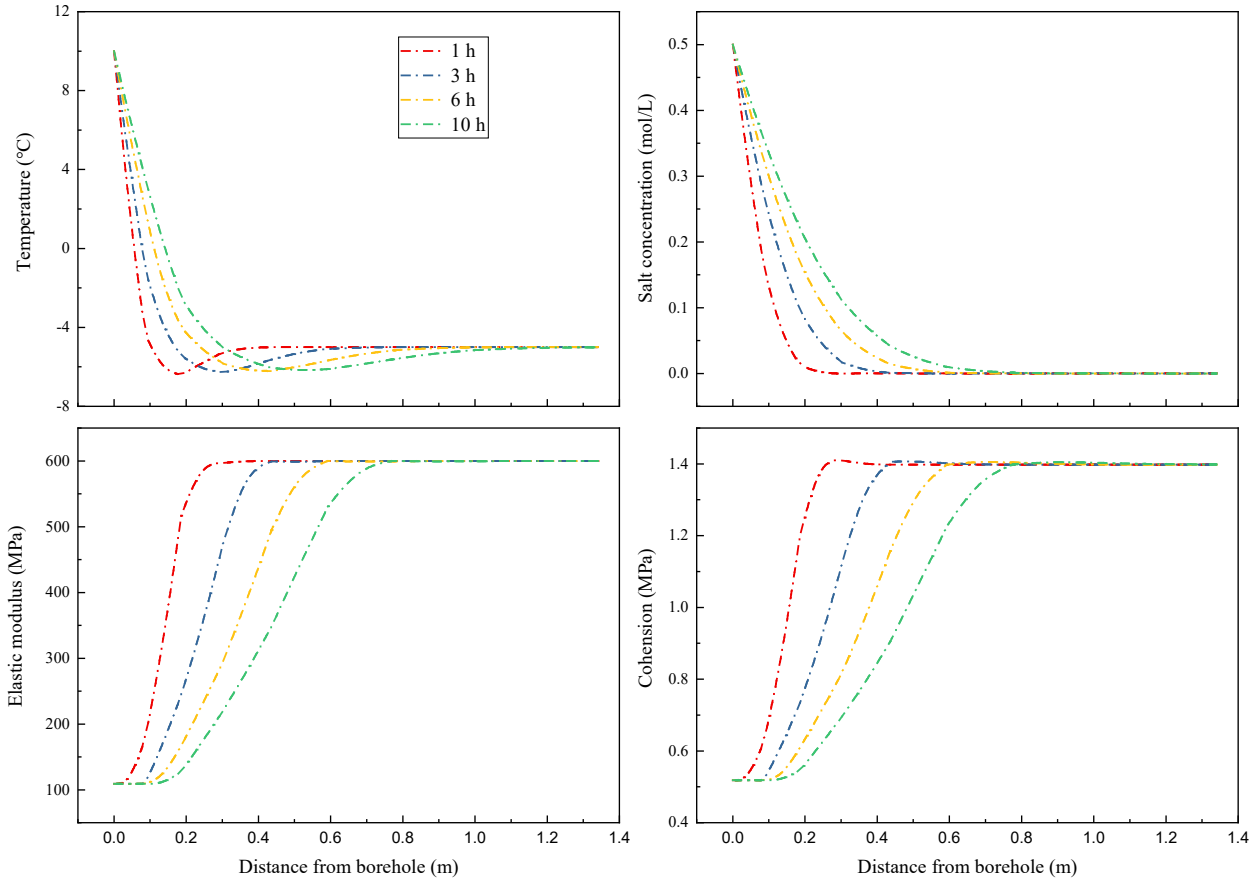

Figure 10. Changes in the temperature field, chemical field, and mechanical properties of the strata after different drilling durations.

Figure 11 illustrates the distributions of the plastic strain and maximum principal stress in the strata in the direction of the minimum horizontal geostress after drilling for different durations. As the drilling duration is prolonged, the plastic deformation around boreholes constantly accumulates, and the area of the plastic yield zones also enlarges, because the area of strata that is affected by the temperature of the drilling fluids constantly increases as the drilling duration increases. In the strata near the boreholes, the mechanical properties of the strata decline because the soils are completely thawed (the blue area in Figure 11), which causes low maximum principal stress. At the same time, the accumulation rate of the plastic deformation of the strata also accelerates, the zone around the boreholes collapses, and the borehole radius expands. In the areas where the pore ice content changes, the secondary stress concentration occurs due to the abrupt changes in the mechanical properties of the strata (the green area in Figure 11), so that the areas that are not completely thawed are also deformed plastically, which is also the cause for the constantly increasing plastic deformation zone in the strata. Figure 12 shows the evolution of the collapsed zones around the boreholes. As the immersion time in the drilling fluids increases, the collapsed zone around the boreholes constantly expands to a location far from the borehole walls.

Affected by the horizontal differential geostress, the collapsed zones of the borehole walls develop in the following two directions: radial and circumferential. The circumferential development of the collapsed zone causes the collapsed zones around the boreholes to coalesce in different directions; the radial development enlarges the area of the collapsed zones, thus constantly increasing the borehole expansion rate. The borehole expansion rate is 8.1% after drilling for 1 h, while it is 24.2% after drilling for 10 h.

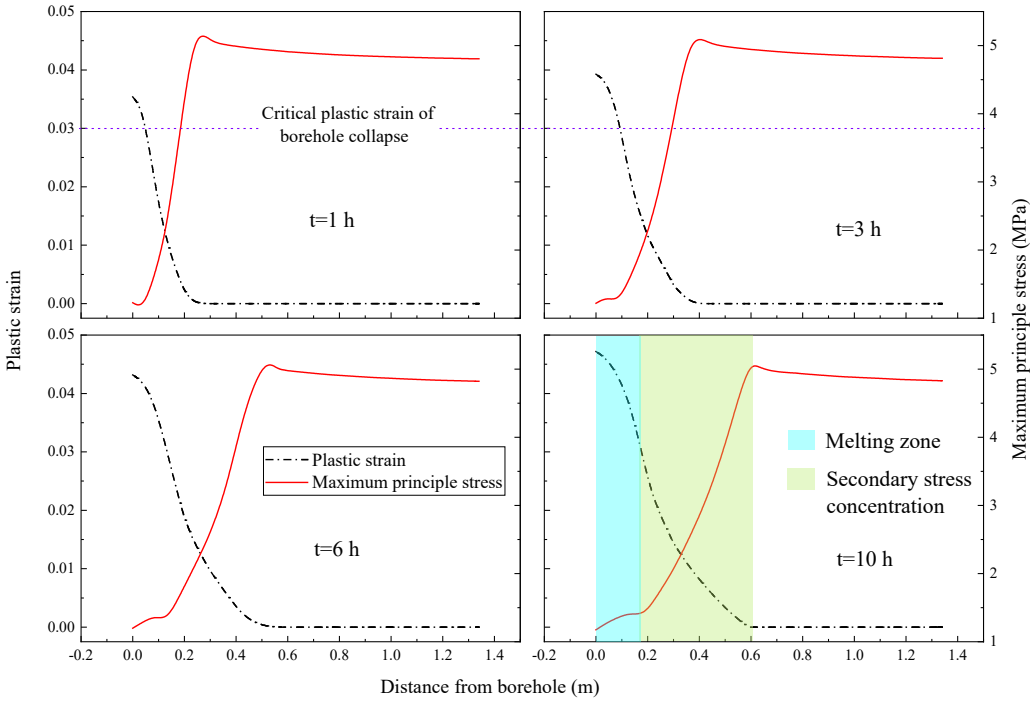

Figure 11. Distributions of the plastic strain and maximum principal stress in the strata in the direction of the minimum horizontal geostress after drilling for different durations.

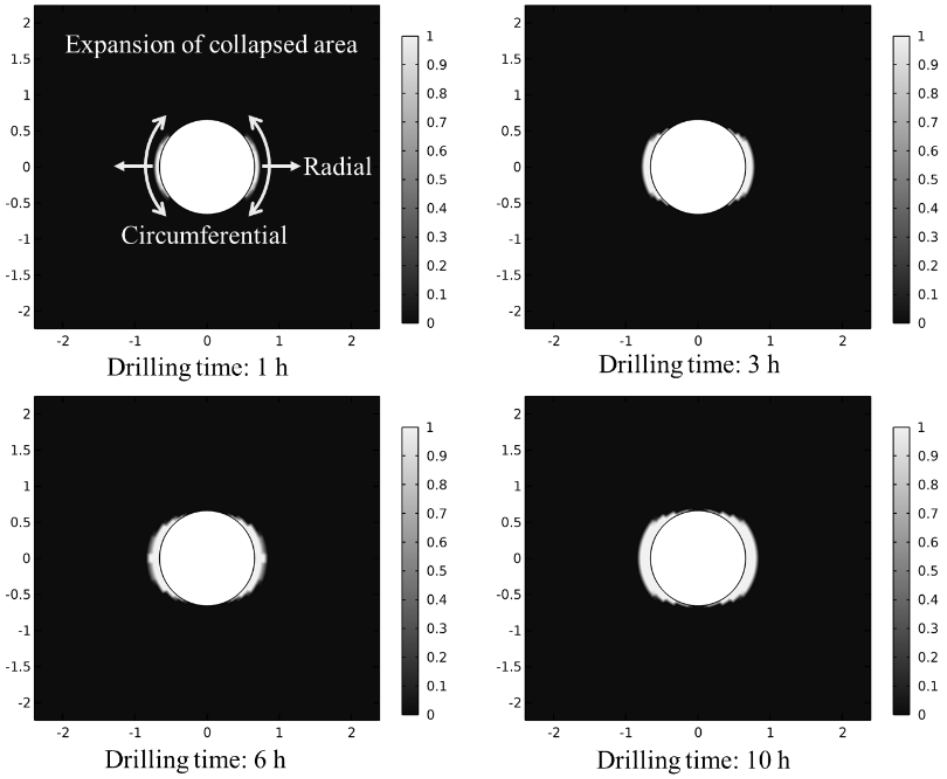

Figure 12. Evolution of the collapsed zones around the boreholes.

5.2. Influences of Temperature of Drilling Fluids

The thawing range of the strata around the boreholes directly affects the collapse degree of the borehole walls. To analyze the influences of the temperature of the drilling fluids on the borehole collapse in the permafrost strata, a model with drilling fluids of 2, 6, 10, and 14 °C is established based on the initial model for comparative analysis. As shown in Figure 13a, the higher the temperature of the drilling fluids, the larger is the heated area in the strata after the same drilling duration. For instance, only those strata 0.045 m from the borehole walls are thawed after drilling the borehole with drilling fluids of 2 °C for 10 h, whereas the thawing range enlarges to 0.167 m from the borehole walls if the temperature of the drilling fluids is 14 °C, leading to a larger area of strata having decreased pore ice content and mechanical properties, as displayed in Figure 13b. For the stability of the borehole walls, the rising temperature of the drilling fluids results in a nonlinear increase in the borehole expansion rate (Figure 14). Under the same conditions, the borehole expansion rates are 0.17, 0.21, and 0.33 when the temperatures of the drilling fluids are 2, 8, and 14 °C, respectively. Therefore, the temperature of the drilling fluids should be decreased if drilling conditions permit, which contributes to shrinking the collapse range. In particular, cyclic cooling of the drilling fluids has a greater effect in maintaining the stability of the borehole walls when the temperature of the drilling fluids is high.

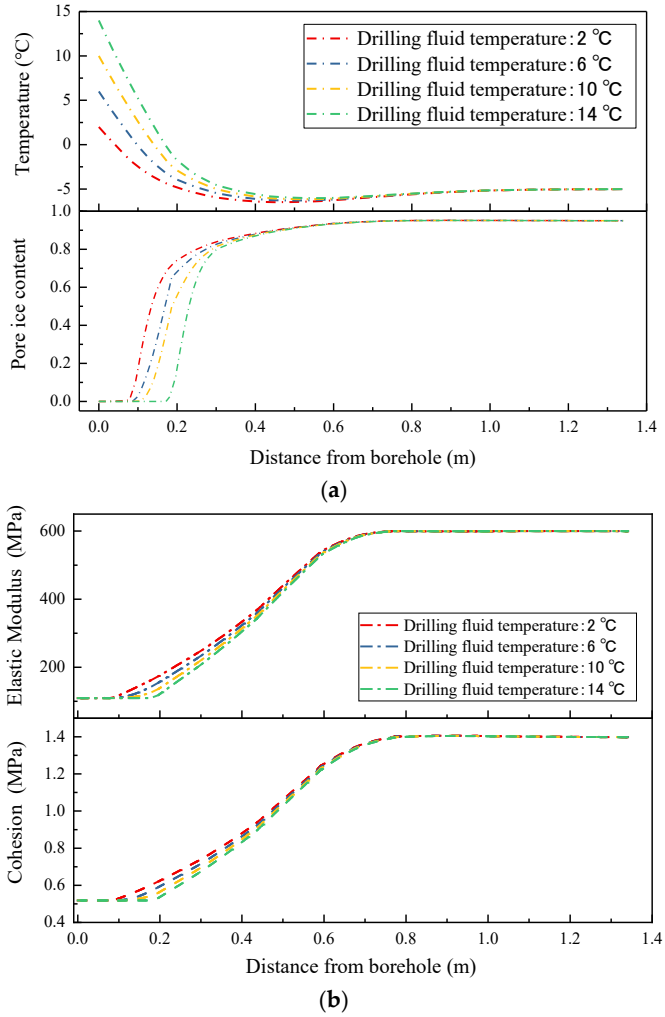

Figure 13. Distributions of the temperature and mechanical properties of the strata around the boreholes at different temperatures of drilling fluids. (**a**) Distributions of the temperature and pore ice content in the strata around the boreholes at different temperatures of drilling fluids. (**b**) Distributions of the mechanical properties of the strata at different temperatures of drilling fluids.

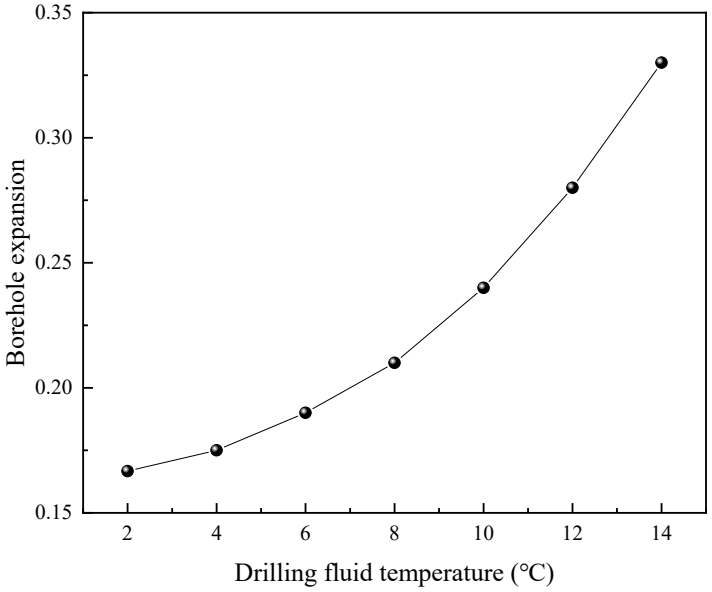

Figure 14. Borehole expansion rates at different temperatures of drilling fluids.

5.3. Influences of Concentrations of Salt Components in Drilling Fluids

The diffusion of salt components in drilling fluids may change the pore ice content in the frozen area of the strata and reduce the mechanical properties of the strata beyond the thawed area. To analyze the influences of the concentration of salt components in drilling fluids on borehole collapse in permafrost strata, a model with salt component concentrations of 0, 0.25, 0.5, and 0.75 mol/L was further built on the basis of the initial model for comparative analysis. The diffusion of salt components in drilling fluids causes the chemical decomposition of the pore ice in the strata around the boreholes. Figure 15 illustrates the distributions of the concentration of salt components, pore ice content, and mechanical properties under different conditions. The higher the concentration of salt components in drilling fluids, the larger is the affected area of pore ice in the strata under the same conditions. However, the overall temperature of the strata decreases due to heat absorption during the decomposition of the ice. For example, the pore ice content and the strata temperature are 0.92 and −2.48 °C, respectively, at a position 0.3 m from the borehole walls after drilling for 10 h with drilling fluids with a concentration of salt components of 0 mol/L. If the concentration of salt components is 0.75 mol/L, the pore ice content is 0.80, and the strata temperature drops to −5.59 °C. The influence of salt components in drilling fluids on the pore ice content in frozen strata can reduce the mechanical properties of the frozen area and significantly change the stress distribution in the strata. Figure 16 depicts the distributions of the maximum principal stress and plastic strain in the strata. The peak secondary stress concentration caused by the abrupt changes in the mechanical properties of the strata with the increasing concentration of salt components in the drilling fluids gradually shifts away from the boreholes and results in a larger collapse range for the borehole walls. For instance, the peak secondary stress concentration is located at the position 0.366 m from the borehole walls if the concentration of salt components in the drilling fluids is 0 mol/L; the peak is 0.63 m from the borehole walls if the concentration of salt components is 0.75 mol/L. The cause for the gradual decrease in the peak strength of the zone is that, the larger the ionic concentration, the larger is the transition zone of the pore ice content, and the smaller is the change gradient. As a result, the area of the plastic yield zone in the strata and the borehole expansion rate increase correspondingly. The borehole expansion rates are 16.7% and 30.3% when the concentrations of salt components in the drilling fluids are 0 and 0.75 mol/L, respectively. The failure risk of the borehole

walls due to the invasion of drilling fluids into the strata can be reduced significantly by decreasing the concentration of salt components in the drilling fluids and using other antifreezing agents, such as alcohols.

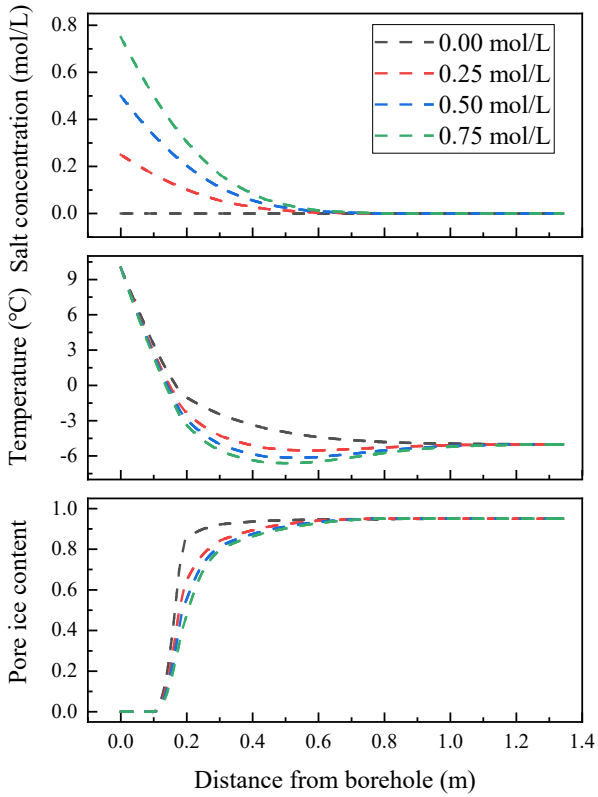

Figure 15. Salt concentration and pore ice content under different concentrations of salt components in drilling fluids.

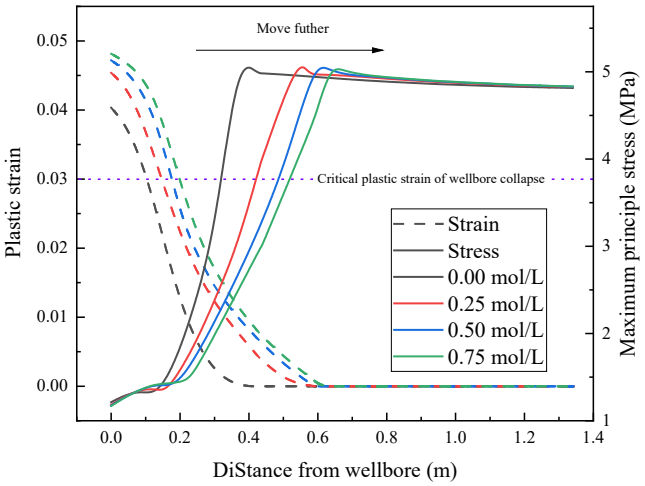

Figure 16. Distributions of the maximum principal stress and the plastic strain under different concentrations of salt components in drilling fluids.

5.4. Influences of Density of Drilling Fluids

The fluid column pressure of drilling fluids can be used to maintain the mechanical stability of the borehole walls. To analyze the influences of the density of drilling fluids on the stability of the boreholes in permafrost strata, a model with drilling fluid densities of 1.00, 1.03, 1.06, and 1.10 g/cm^3 was further established on the basis of the initial model for comparative analysis. Figure 17a illustrates the collapse ranges of the borehole walls under

different densities of drilling fluids. As the density of the drilling fluids rises, the collapse degree of the borehole walls greatly decreases. For example, the borehole expansion rates are 26.7% and 15.4% when the densities of the drilling fluids are 1.00 and 1.10 g/cm^3, respectively, because increasing the density of the drilling fluids can improve the stress level of the strata around the boreholes, as displayed in Figure 17b. Increasing the density of the drilling fluids can increase the differential stress between the fluid column pressure of the drilling fluids in the boreholes and the pore pressure in the strata. Despite this factor, it does not intensify the heat transfer and diffusion of the salt components in the drilling fluids to the strata due to the extremely low permeability of the permafrost and the insignificant convection, which differs from other strata that are affected by the mass and heat transfer effects of the drilling fluids, such as hydrate formation (Wei et al., 2019 [27]). Therefore, although mass and heat transfer effects exist between the drilling fluids and the strata in the drilling process in permafrost strata, increasing the density of the drilling fluids can greatly improve the stability of the borehole walls.

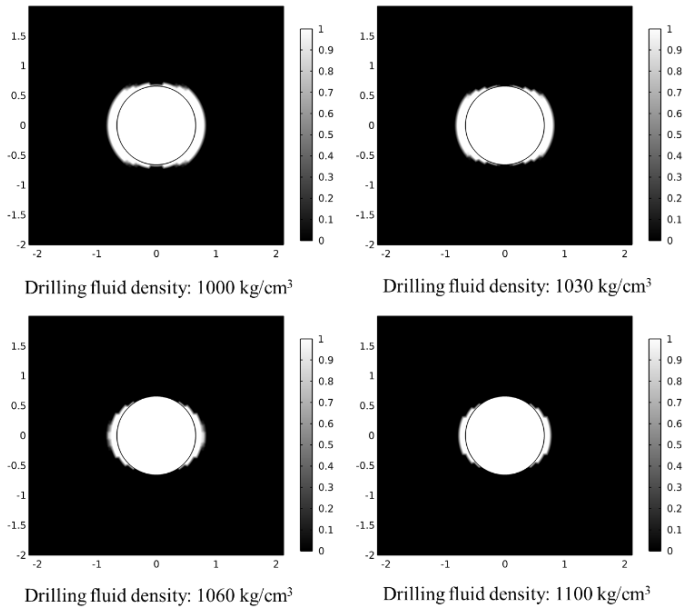

(**a**)

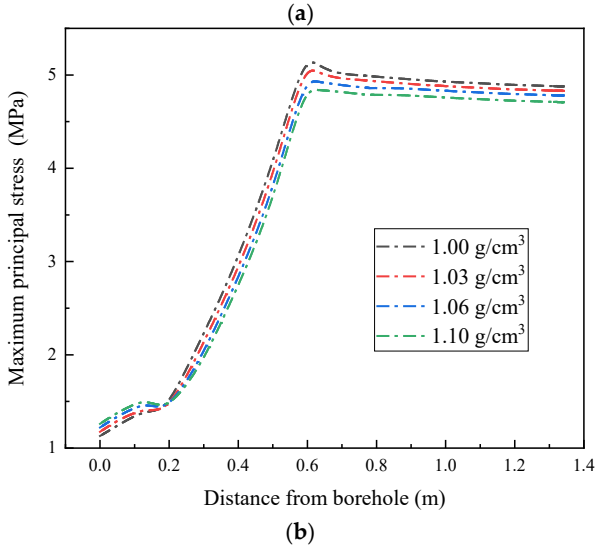

(**b**)

Figure 17. Distributions of the collapse of the borehole walls and the maximum principal stress under different densities of drilling fluids. (**a**) Collapse range of the borehole walls under different densities of drilling fluids. (**b**) Distribution of the maximum principal stress in the strata under different densities of drilling fluids.

6. Conclusions

The heat conduction of drilling fluids to strata directly determines the thawing range of permafrost. The diffusion of salt components influences the freezing temperature of pore water and the pore ice content in the frozen area. The heat and salt components of drilling fluids cannot be transferred through convection, which can be ignored.

The reduction in the mechanical properties of the strata in the thawed area of permafrost renders the stress at a low level and accelerates the accumulation rate of plastic deformation in the strata. In the frozen area where the pore ice content changes, the abrupt change in the mechanical properties of the strata causes the secondary stress concentration, so that plastic deformation also occurs in the strata that are not completely thawed. As the drilling duration is prolonged, the range of the strata affected by the mass and heat transfer effects of the drilling fluids constantly expands, and the collapsed zones of the borehole walls develop in the radial and circumferential directions. Circumferential development contributes to the coalescence of the collapsed zones in different directions; radial development enlarges the range of the collapsed zones, thus increasing the borehole expansion rate.

As the drilling fluid temperature decreases, the borehole expansion rate subsequently shows a nonlinear decrease. An increase in the concentration of salt components in the drilling fluid will result in peaks of secondary stress concentrations that will progressively move away from the borehole and lead to a greater range of plastic yielding. Increasing the drilling fluid density will not exacerbate the mass and heat transfer from the drilling fluid to the formation, but it will greatly affect the stress distribution in the formation, reduce the extent of borehole collapse, and improve the stability of the borehole.

Author Contributions: Formal analysis, Q.C.; Investigation, J.S. and L.S.; Writing—original draft, Y.L. All authors have read and agreed to the published version of the manuscript.

Funding: This work was financially supported by the National Key Research and Development Program of China (2022YFC2806400).

Data Availability Statement: Some or all of the data, models, or code that support the findings of this study are available from the corresponding author upon reasonable request.

Conflicts of Interest: Author Yang Li was employed by Sinopec Research Institute of Petroleum Engineering Co., Ltd. Authors Jihui Shi and Qiang Cui were employed by Sinopec Shanghai Offshore Oil & Gas Company. The remaining author declares that the research was conducted in the absence of any commercial or financial relationships that could be construed as a potential conflict of interest.

References

1. Wei, N.; Pei, J.; Li, H.; Zhou, S.; Zhao, J.; Kvamme, B.; Coffin, R.B.; Zhang, L.; Zhang, Y.; Xue, J. Classification of natural gas hydrate resources: Review, application and prospect. *Gas Sci. Eng.* **2024**, *124*, 205269. [CrossRef]
2. Huang, Y.; Li, X.; Liu, X.; Zhai, Y.; Fang, F.; Guo, W.; Qian, C.; Han, L.; Cui, Y.; Jia, Y. Review of the productivity evaluation methods for shale gas wells. *J. Pet. Explor. Prod. Technol.* **2024**, *14*, 25–39. [CrossRef]
3. Wang, P.; Zhang, X.; Zhu, Y.; Li, B.; Huang, X.; Pang, S.; Zhang, S.; Lu, C.; Xiao, R. Effect of permafrost properties on gas hydrate petroleum system in the Qilian Mountains, Qinghai, Northwest China. *Environ. Sci. Process. Impacts* **2014**, *16*, 2711–2720. [CrossRef]
4. Bird, K.J.; Charpentier, R.R.; Gautier, D.L.; Houseknecht, D.W.; Klett, T.R.; Pitman, J.K.; Moore, T.E.; Schenk, C.J.; Tennyson, M.E.; Wandrey, C.R. *Circum-Arctic Resource Appraisal: Estimates of Undiscovered Oil and Gas North of the Arctic Circle*; US Geological Survey Fact Sheet 2008-3049; US Geological Survey: Baltimore, MD, USA, 2008; 4p.
5. Li, Y.; Cheng, Y.; Yan, C.; Xue, M.; Niu, C.; Gao, Y.; Wang, T. Simulating the effect of frozen soil thaw on wellhead stability during oil and gas drilling operations in arctic waters. *J. Cold Reg. Eng.* **2020**, *34*, 04020026. [CrossRef]
6. Zhang, S.; Kuang, H.; Jin, Z.; Xu, G. An experimental study of the stress-strain characteristics of frozen silty clay with high moisture content. *Hydrogeol. Eng. Geol.* **2020**, *47*, 116–124.
7. Sun, K.; Tang, L.; Zhou, A.; Ling, X. An elastoplastic damage constitutive model for frozen soil based on the super/subloading yield surfaces. *Comput. Geotech.* **2020**, *128*, 103842. [CrossRef]

8. Yakushev, V.S. Permafrost impact on gas fields development in the Russian onshore Arctic (Yamal Peninsula). In Proceedings of the OTC Arctic Technology Conference, Copenhagen, Denmark, 23–25 March 2015. OTC-25504-MS.
9. Li, Y.; Cheng, Y.F.; Yan, C.L.; Wang, Z.Y.; Song, L.F. Effects of creep characteristics of natural gas hydrate-bearing sediments on wellbore stability. *Pet. Sci.* **2021**, *19*, 220–233. [CrossRef]
10. Li, Y.; Cheng, Y.; Yan, C.; Song, L.; Zhou, X.; Niu, C. Influence of drilling fluid temperature on borehole shrinkage during drilling operation in cold regions. *J. Pet. Sci. Eng.* **2020**, *190*, 107050. [CrossRef]
11. Perkins, T.K.; Rochon, J.A.; Knowles, C.R. Studies of pressures generated upon refreezing of thawed permafrost around a wellbore. *J. Pet. Technol.* **1974**, *26*, 1159–1166. [CrossRef]
12. Wang, K. Simulation and Analysis of Wellbore Stability in Permafrost Formation with FLAC. Master's Thesis, University of Alaska Fairbanks, Fairbanks, AK, USA, 2015.
13. Wang, X.; Wang, Z.; Deng, X.; Sun, B.; Zhao, Y.; Fu, W. Coupled thermal model of wellbore and permafrost in Arctic regions. *Appl. Therm. Eng.* **2017**, *123*, 1291–1299. [CrossRef]
14. Kutasov, I.M.; Eppelbaum, L.V. Time of refreezing of surrounding the wellbore thawed formations. *Int. J. Therm. Sci.* **2017**, *122*, 133–140. [CrossRef]
15. Li, Y.; Yan, C.; Cheng, Y.; Han, S.C.; Gao, Q.; Wei, J. Numerical simulation of wellbore stability in frozen soil during drilling operation. In Proceedings of the 53rd US Rock Mechanics/Geomechanics Symposium, New York, NY, USA, 23–26 June 2019.
16. Eppelbaum, L.V.; Kutasov, I.M. Well drilling in permafrost regions: Dynamics of the thawed zone. *Polar Res.* **2019**, *38*, 1–9. [CrossRef]
17. Wang, Z.; Sun, J.; Huang, X.; Lv, K.; Geng, Y. A temperature-sensitive polymer with thinner effect as a rheology modifier in deepwater water-based drilling fluids. *J. Mol. Liq.* **2024**, *393*, 123536. [CrossRef]
18. Deng, X.; Pan, S.; Wang, Z.; Ke, K.; Zhang, J. Application of the Darcy-Stefan model to investigate the thawing subsidence around the wellbore in the permafrost region. *Appl. Therm. Eng.* **2019**, *156*, 392–401. [CrossRef]
19. Razali, S.Z.; Yunus, R.; Rashid, S.A.; Lim, H.; Jan, B.M. Review of biodegradable synthetic-based drilling fluid: Progression, performance and future prospect. *Renew. Sustain. Energy Rev.* **2018**, *90*, 171–186. [CrossRef]
20. Liang, L.; Xiong, J.; Liu, X. Experimental study on crack propagation in shale formations considering hydration and wettability. *J. Nat. Gas Sci. Eng.* **2015**, *23*, 492–499. [CrossRef]
21. Wang, Z.; Sun, Y.; Li, Z.; Wang, Y.; You, Z. Multiphysics responses of coal seam gas extraction with borehole sealed by active support sealing method and its applications. *J. Nat. Gas Sci. Eng.* **2022**, *100*, 104466. [CrossRef]
22. Wang, Q.; Chen, Z.; Ma, P.; Jiang, Y. Analysis of effect factor in shale wellbore stability. In Proceedings of the 47th US Rock Mechanics/Geomechanics Symposium, San Francisco, CA, USA, 23–26 June 2013.
23. Sun, J.; Ning, F.; Lei, H.; Gai, X.; Sánchez, M.; Lu, J.; Li, Y.; Liu, L.; Liu, C.; Wu, N.; et al. Wellbore stability analysis during drilling through marine gas hydrate-bearing sediments in Shenhu area: A case study. *J. Pet. Sci. Eng.* **2018**, *170*, 345–367. [CrossRef]
24. Li, Y.; Cheng, Y.; Yan, C.; Song, L.; Liu, H.; Tian, W.; Ren, X. Mechanical study on the wellbore stability of horizontal wells in natural gas hydrate reservoirs. *J. Nat. Gas Sci. Eng.* **2020**, *79*, 103359. [CrossRef]
25. Wang, H.N.; Chen, X.P.; Jiang, M.J.; Guo, Z.Y. Analytical investigation of wellbore stability during drilling in marine methane hydrate-bearing sediments. *J. Nat. Gas Sci. Eng.* **2019**, *68*, 102885. [CrossRef]
26. Harlan, R.L. Analysis of coupled heat-fluid transport in partially frozen soil. *Water Resour. Res.* **1973**, *9*, 1314–1323. [CrossRef]
27. Wei, J.; Cheng, Y.; Yan, C.; Li, Q.; Han, S.; Ansari, U. Decomposition prevention through thermal sensitivity of hydrate formations around wellbore. *Appl. Therm. Eng.* **2019**, *159*, 113921. [CrossRef]
28. Li, Y.; Cheng, Y.; Yan, C.; Wang, Z.; Zhang, Q.; Zhou, P. Stratum Settlement during Depressurization of Horizontal Wells in Gas Hydrate Reservoirs. *Energy Fuels* **2021**, *35*, 14692–14708. [CrossRef]
29. Taylor, G.S.; Luthin, J.N. A model for coupled heat and moisture transfer during soil freezing. *Can. Geotech. J.* **1978**, *15*, 548–555. [CrossRef]
30. Meng, X.; Zhou, J.; Wei, C.; Zhang, K.; Shen, Z.; Yang, Z. Effects of salinity on soil freezing temperature and unfrozen water content. *Rock Soil Mech.* **2020**, *41*, 952–960.
31. Ghassemi, A.; Zhang, Q. A transient fictitious stress boundary element method for porothermoelastic media. *Eng. Anal. Bound. Elem.* **2004**, *28*, 1363–1373. [CrossRef]
32. Li, S.; Zhang, M.; Pei, W.; Lai, Y. Experimental and numerical simulations on heat-water-mechanics interaction mechanism in a freezing soil. *Appl. Therm. Eng.* **2018**, *132*, 209–220. [CrossRef]